Title
Ultrahigh quality van der Waals hyperbolic polariton resonators

Authors
Yu, Shang-Jie
Jiang, Yue
Roberts, John A
et al.

Publication Date
2022-03-05

DOI
10.1117/12.2612301

Peer reviewed

Ultrahigh-quality van der Waals hyperbolic polariton resonators

Shang-Jie Yu[1], Yue Jiang[1], John A. Roberts[1], Markus A. Huber[1], Helen Yao[1], Xinjian Shi[1], Hans A. Bechtel[2], Stephanie N. G. Corder[2], Tony F. Heinz[1], Xiaolin Zheng[1], and Jonathan A. Fan[1]*

1. Stanford University, Stanford, CA, USA

2. Lawrence Berkeley National Laboratory, Berkeley, CA, USA

** jonfan@stanford.edu*

Abstract: We demonstrate the growth, assembly, and characterization of ultrahigh quality polaritonic systems based on α-MoO_3 microplates and nanoribbons. These micro- and nanostructures are bottom-up-synthesized single crystals with minimal impurities. By optimizing the growth conditions, we also realize morphology control of the α-MoO_3 structures. We observe highly confined polariton modes in the individual structures by using scattering-type scanning near-field optical microscopy and nanospectroscopy. These highly confined polariton modes are of fundamental and technological interest.

1. Introduction

In the infrared wavelength range, van der Waals (vdW) materials have emerged as an exciting and heavily studied class of materials due to their ability to support exceptionally high-quality phonon polariton (PhP) excitations, which occur in the Reststrahlen bands (RBs) between the longitudinal optical and corresponding transverse optical phonon frequencies. These vdW polaritonic systems include h-BN, α-MoO_3, and α-V_2O_5, and they have been a testbed for evaluating light-matter interactions ranging from hyperbolic dispersion to strong coupling phenomena and also inspired new concepts and regimes in sensing, imaging, and waveguiding.

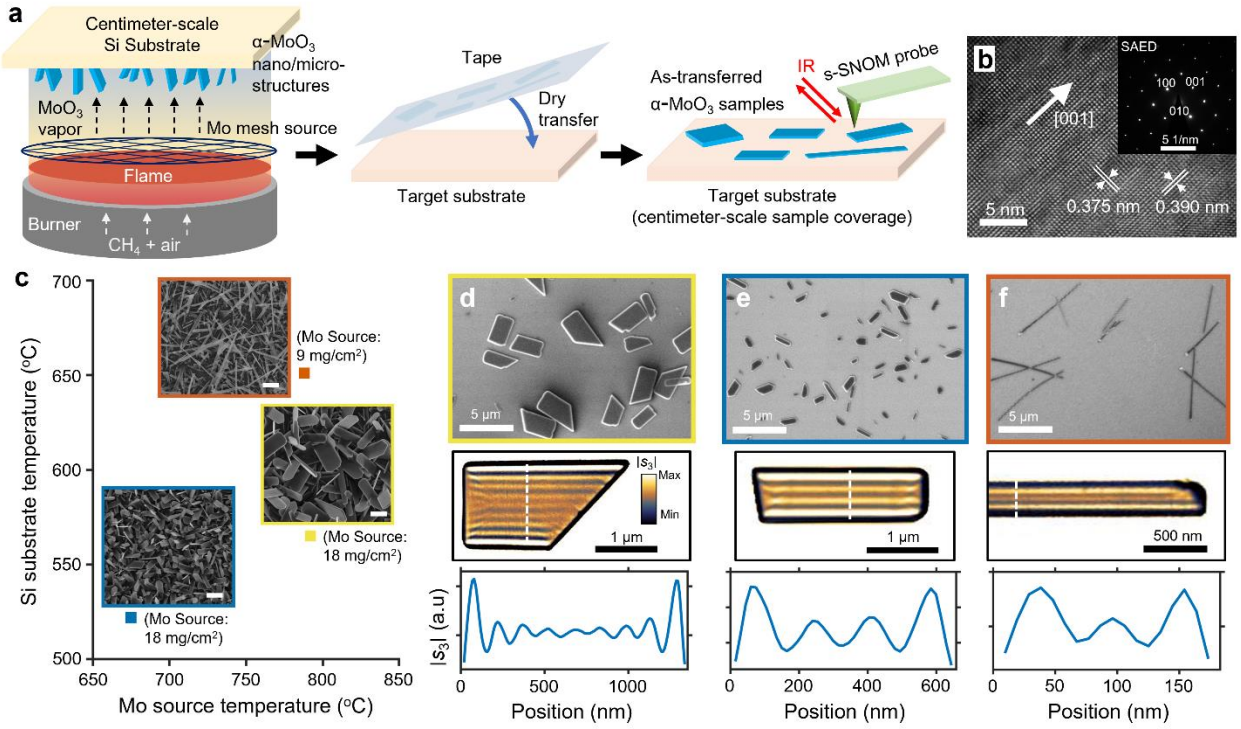

Figure 1. **α-MoO3 sample preparation, morphology control, and characterization.** **a**, FVD setup and materials preparation workflow, including flame synthesis, direct dry transfer, and near-field optical characterization of as-transferred α-MoO_3 structures. **b**, HRTEM image of a representative α-MoO_3 structure. Inset: SAED pattern. **c**, Morphology control of α-MoO_3 nano- and micro-structures by varying the FVD conditions. SEM images of as-grown α-MoO_3 are shown for each synthesis condition. Scale bars: 1 μm. **d-f**, Top row: SEM images of as-transferred samples on SiO_2/Si substrates prepared under different FVD conditions. Yellow, dark blue and dark red boxes indicate (**d**) microplates, (**e**) low-aspect-ratio nanoribbons, and (**f**) high-aspect-ratio nanoribbons, respectively. Middle row: corresponding s-SNOM images of an individual microplate and nanoribbons recorded at 931 cm^{-1}. Bottom row: near-field amplitude ($|s_3|$) profiles taken from the cross-sections of the middle-row images, denoted by the dashed lines.

α-MoO_3 is a particularly unique vdW phonon polaritonic material as it exhibits biaxial anisotropy[1], which enables IR polarization conversion and in-plane hyperbolic PhP modes. More recently, topological photonic dispersion engineering was demonstrated in twisted bilayer α-MoO_3 structures, providing a new avenue towards flexible polaritonic tuning and routing.

In this work, we demonstrate the growth, assembly, and characterization of ultrahigh quality polaritonic systems based on α-MoO_3 microplates and nanoribbons, synthesized using the flame vapor deposition (FVD) method[2]. FVD is a versatile platform for growing nanostructured metal oxides and is noteworthy for its rapid growth rates, low cost, high scalability, and use of atmospheric operation conditions. FVD synthesized α-MoO_3 combines multiple features in materials preparation that enables unprecedented optical properties. First, FVD-grown structures are crystalline with minimal impurities, and they have material properties consistent with flakes exfoliated from bulk single crystals. Second, α-MoO_3 nanoribbons have smooth and parallel edges, naturally forming ideal Fabry-Pérot (FP) phonon polaritonic resonators without the need for nanopatterning. Third, as-grown structures can be easily transferred to any solid substrate with minimal contamination.

2. Design Method and Results

We synthesize and prepare high-quality α-MoO_3 nano- and micro-structures using the workflow illustrated in Figure 1a. Using FVD, we grow stoichiometric and single-crystalline α-MoO_3 structures. The as-grown α-MoO_3 is then transferred to a flat target substrate using low-adhesion tape and probed by scattering-type scanning near-field optical microscopy (s-SNOM), which is an established tool for infrared PhP study. α-MoO_3 has multiple RBs in FIR and MIR spectral range and supports broadband hyperbolic phonon polaritons[2].

We probe the crystallinity and phase of as-grown MoO_3 structures using high-resolution transmission electron microscopy (HRTEM) and selected area electron diffraction (SAED), which confirm that the structures are crystalline orthorhombic α-MoO_3, the preferred growth direction is [001], and the out-of-plane orientation is [010] (Figure 1b).

We also realize morphology control of the α-MoO_3 structures by adjusting the FVD growth conditions. With the growth temperature and area density variations, we can reproducibly synthesize α-MoO_3 with three different morphologies (Figure 1c): microplates, low-aspect-ratio nanoribbons, and nanowires. s-SNOM images of individual α-MoO_3 structures grown under different conditions (Figure 1d-f) and taken within RB_Y show distinct PhP behaviors. The microplates, which have widths longer than the PhP propagation distance, show long-range PhP propagation with exponentially decaying envelopes. The nanoribbons and nanowires, on the other hand, have widths much shorter than the PhP propagation distance and serve as FP resonators[3,4] that support PhP standing waves.

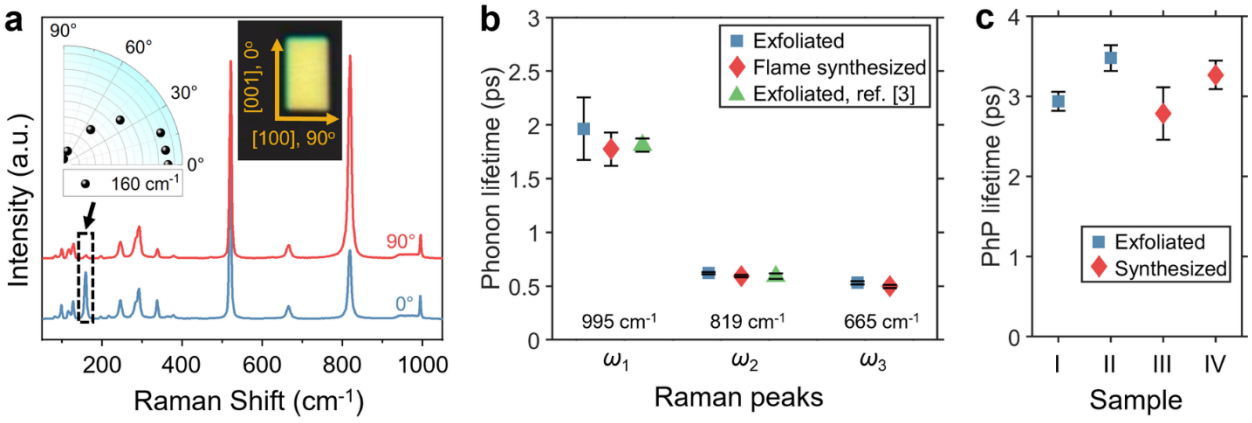

Figure 2. **Raman spectroscopy and phonon lifetime.** **a**, Raman spectra of a microplate with the excitation light polarized along the long edge (0°) and the short edge (90°). Left-top inset: the excitation polarization dependence of Raman peak at 160 cm^{-1} showing in-plane anisotropy. Right-top inset: optical image of the microplate characterized by Raman spectroscopy. The arrows denote the crystal axes and polarization angle. **b**, Phonon lifetimes of exfoliated and flame synthesized samples, extracted from the Raman spectra. The first dataset is collected on 12 exfoliated flakes, the second dataset is on 22 flame-synthesized microplates and nanoribbons, and the third dataset is on 6 exfoliated flakes from Ref. [1]. The labels ω_1, ω_2, and ω_3 correspond to the phonon lifetime data of the Raman peaks at 995 cm^{-1}, 819 cm^{-1}, and 665 cm^{-1}, respectively. Data from the 665 cm^{-1} peak are not available for the third dataset. The error bars denote standard deviations for phonon lifetime evaluation from Raman peak fitting. **c**, PhP lifetimes of exfoliated and flame synthesized samples, extracted from s-SNOM imaging at 939 cm^{-1}. The error bars show the standard deviations from fitting.

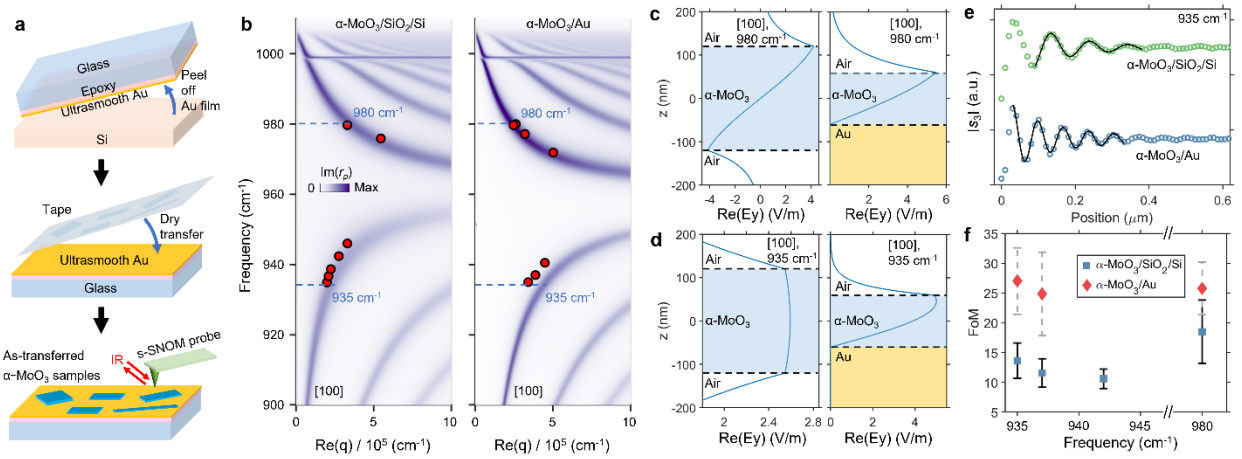

Figure 3. PhP mode dispersion and figure of merit. **a**, Material preparation workflow, including ultrasmooth gold template stripping, direct dry transfer, and s-SNOM characterization of as-transferred α-MoO_3 samples. **b**, Left: PhP dispersion of 112 nm-thick α-MoO_3 on SiO_2, with in-plane momentum q along [100]. The points are experimental data for microplates on 90 nm SiO_2/Si. Right: PhP dispersion of 120 nm-thick α-MoO_3 on gold, with q along [100]. The points are the corresponding experimental data on ultrasmooth gold. **c-d**, Calculated electric field profiles in the vertical cross-sections of guided modes along [100] direction in air/240 nm thick α-MoO_3/air and air/120 nm thick α-MoO_3/gold at (**c**) 980 cm^{-1} and (**d**) 935 cm^{-1}. The y-axis is in the out-of-plane direction (*i.e.*, normal to plot plane). **e**, Typical s-SNOM fringe traces on α-MoO_3/SiO_2/Si and α-MoO_3/ultrasmooth gold samples imaged at 935 cm^{-1}. The circles are experimental data and the black lines are fitting curves. **f**, Figure of merit (FoM), defined as Re(q)/Im(q), of PhPs measured from various microplates on SiO_2 and ultrasmooth gold, evaluated by fitting s-SNOM fringe traces.

To quantify the quality of the phonon resonances in FVD-grown α-MoO_3 microplates with optical metrology methods, we utilize a combination of Raman spectroscopy and s-SNOM methods. With Raman spectroscopy, we can directly probe the in-plane anisotropic Raman response and extract the phonon lifetimes from the peak width. Representative Raman spectra for structures on oxidized silicon substrates are plotted in Figure 2a and display a strong dependence on the pump light polarization with respect to the ribbon crystal axis at 160 cm^{-1}, which is attributed to anisotropic lattice vibrations within the vdW α-MoO_3 plane. This result confirms the direction of ribbon growth. We also quantify the phonon lifetimes of Raman active modes at 995 cm^{-1} and 818 cm^{-1} from the microplates and compare them with exfoliated flakes from bulk single crystals. The results from this benchmark comparison are summarized in Figure 2b and show that the lifetimes from both materials are similar and consistent with previously published data on exfoliated flakes. The PhP lifetimes from FVD-grown and exfoliated samples are also quantified by s-SNOM and produce values consistent with the Raman analysis. All these results indicate that our FVD-grown structures have comparable crystal quality with ideal single crystal samples prepared by bulk exfoliation.

To further engineer the α-MoO_3 PhP propagation mode in a scalable manner that eliminates phonon-polariton interactions with the underlying substrate, we tape-transfer α-MoO_3 microplates onto freshly template-stripped ultrasmooth gold substrates (Figure 3a). Our use of ultrasmooth gold substrates offers several advantages. First, the elimination of phonon contributions from the underlying substrate removes ambiguity involving the source of PhPs across the full infrared frequency range and mitigates modal absorption from coupling to substrate phonons. While gold does introduce free carrier absorption, this absorption contribution is minimal at mid- and far-infrared (FIR) wavelengths in our system (see Supporting Information). Second, freshly template-stripped gold has surface roughness on the angstrom scale and therefore contributes negligible surface scattering, which is critical to minimizing losses during PhP propagation. Evaporated or sputtered gold substrates, which have been previously used in h-BN device studies, are rougher and contribute greater surface scattering loss. Third, the gold substrate at infrared frequencies enforces mirror-like electromagnetic boundary conditions at the gold-microplate interface, leading to minimal field penetration into the substrate and strong tailoring of mode confinement and mode symmetry properties.

We study the dispersion of α-MoO_3 microplates on ultrasmooth metal substrates and compare the results with microplates on SiO_2/Si substrates. The PhP momenta are extracted through s-SNOM imaging. The results (Figure 3b) show good agreement between experimental and theoretical curves and display clear spatial mode compression near the α-MoO_3 phonon resonance, with wavelength compression as large as $\lambda/50$. Notably, as the substrate changes from SiO_2/Si to gold, the upper RB dispersion curve shifts towards lower momentum while the lower RB dispersion curve shifts towards higher momentum. This dispersion dependence on substrate material can be understood in the context of mode symmetry. In the metal-substrate system, the gold surface enforces an electric field node at the α-

MoO_3-metal interface, such that the electromagnetic modes take the form of anti-symmetric modes in an air-clad α-MoO_3 film with a doubled thickness (Figure 3c and 3d). The enforcement of anti-symmetry in the mode profiles therefore serves as a filter that eliminates the presence of symmetric modes in the air-clad α-MoO_3 picture.

We next study the FP PhP modes within the RBs of an α-MoO_3 nanostructure using FIR and MIR ultrabroadband synchrotron infrared nanospectroscopy (SINS). FIR SINS covers the four α-MoO_3 RBs spanning 440 – 1020 cm^{-1} and MIR SINS enables scans with high spectral resolution due to its higher MIR photon detection sensitivity. These nanospectroscopy maps can be directly used to quantify the spectral characteristics of different FP modes in the nanoribbon, which are selectively excited and collected as a function of the probe's location on the resonator (Figure 4a). The experimental and theoretical results (Figure 4) show good agreement.

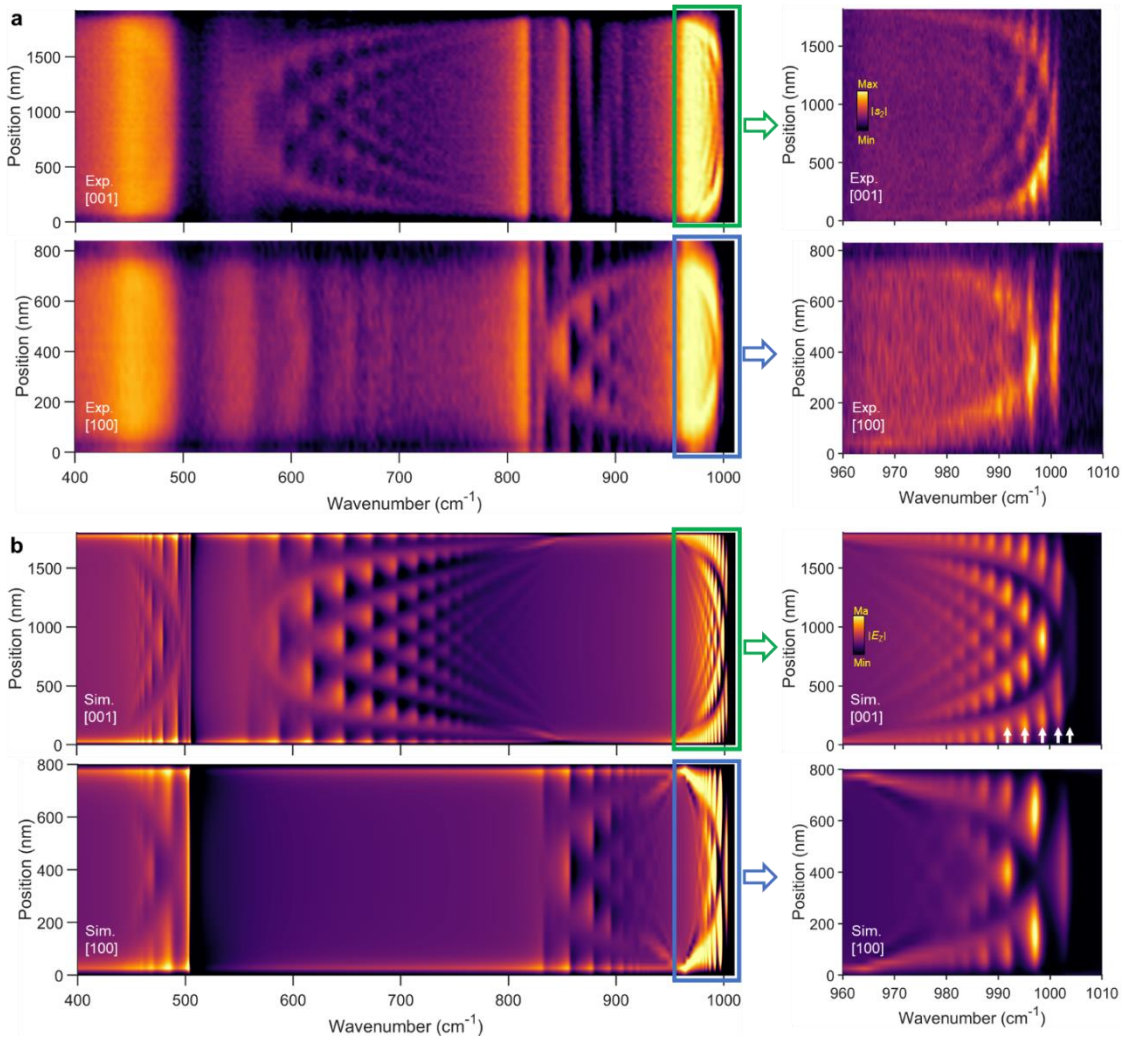

Figure 4. Nanospectroscopy of α-MoO_3 nanoribbon on ultrasmooth gold. **a**, (Left) FIR SINS line scans along [001] (top) and [100] (bottom) across the nanoribbon. (Right) High-resolution MIR SINS line scans along [001] (top) and [100] (bottom) across the nanoribbon. **b**, (Left) Simulated spectra along [001] (top) and [100] (bottom). (Right) Zoom-in of the simulated spectra.

References

1. Ma, W. *et al.* In-plane anisotropic and ultra-low-loss polaritons in a natural van der Waals crystal. *Nature* **562**, 557–562 (2018).
2. Yu, S.-J. *et al.* Ultrahigh-quality infrared polaritonic resonators based on bottom-up-synthesized van der Waals nanoribbons. *ACS Nano* (2022) doi:10.1021/acsnano.1c10489.
3. Roberts, J. A. *et al.* Tunable hyperbolic metamaterials based on self-assembled carbon nanotubes. *Nano Lett.* **19**, 3131–3137 (2019).
4. Roberts, J. A. *et al.* Multiple tunable hyperbolic resonances in broadband infrared carbon-nanotube metamaterials. *Phys. Rev. Appl.* **14**, 044006 (2020).